


# O-carboxymethyl chitosan/gelatin/ silver-copper hydroxyapatite composite films with enhanced antibacterial and wound healing properties

Journal of Biomaterials Applications  
 2022, Vol. 37(5) 773–785  
 © The Author(s) 2022  
 Article reuse guidelines:  
[sagepub.com/journals-permissions](https://sagepub.com/journals-permissions)  
 DOI: 10.1177/08853282221121879  
[journals.sagepub.com/home/jba](https://journals.sagepub.com/home/jba)  


Laura-E Valencia-Gómez<sup>1</sup>, Elia-M Muzquiz-Ramos<sup>2</sup> , Abril-D Fausto-Reyes<sup>1</sup>,  
 Priscila-I Rodríguez-Arellano<sup>1</sup>, Claudia-A Rodríguez-González<sup>1</sup>,  
 Juan-F Hernández-Paz<sup>1</sup>, Hortensia Reyes-Blas<sup>1</sup> and Imelda Olivas-Armendáriz<sup>1</sup> 

## Abstract

Wound dressing composite films of O-carboxymethyl chitosan (OCMC) and gelatin were prepared and mixed with hydroxyapatite (HA) composited with Silver (Ag) and Copper (Cu) at different concentrations. The chemical, thermal, morphological, and biological properties of the composite films were studied. The analysis by FTIR confirmed the presence of interactions between gelatin and OCMC, and at the same time, the polymer matrix interactions with Ag-Cu/HA complex. The inclusion of nanoparticle to the composite was associated with an improvement of the thermal stability, morphological roughness, a 9–12% more hydrophobic behavior (composite C1, C5, and C8), increase in antibacterial activity from 23.2 to 33.1% for gram negative bacteria and from 37.28 to 40.59% for gram positive bacteria, and with a cell viability greater than 100% for 24 and 72 h. The films obtained can serve as a wound healing dressing and regenerating biomaterial.

## Keywords

Polymer-matrix composite, carboxymethyl chitosan, hydroxyapatite, gelatin, silver particles, copper particles

## Introduction

Despite the research in wound healing area and progress in reducing the recurrence rate of infections during epithelial tissue regeneration, current films still struggle to address infection, thereby preventing rapid tissue healing causing complications that can have serious consequences. The development of new films with the ability to fine tune different properties through the inclusion of materials with bioactive and antibacterial properties is necessary.

Nowadays, the solubility of chitosan can be improved by the carboxymethylation reaction, where the hydrophilic modification yields the carboxymethyl chitosan (CMC) polymer. The CMC is a biomaterial that has found numerous medical uses such as regenerative material, drug delivery systems, antibacterial and wound healing films, among others.<sup>1,2</sup> Carboxymethylation reaction occurs mostly at Carbon 6 in the hydroxyl groups (OH) or the amino groups (NH<sub>2</sub>) of the cyclic chain of chitosan, producing N or O-carboxymethyl chitosan compounds (NCMC and OCMC) that are water-soluble at neutral pH.<sup>1,3</sup>

Therefore, OCMC and NCMC are chitosan derivatives with good properties for film formation, as such: elevated viscosity, non-toxicity, and useful biocompatibility. Also, due to the high carboxymethyl groups in all their polymer structure, these chitosan derivatives have upper water solubility, regeneration tissue, and biodegradability when compared to chitosan.<sup>4</sup>

Gelatin polymer is obtained by degraded reaction for collagen. It is obtained from the connective tissues of the

<sup>1</sup>Universidad Autónoma de Ciudad Juárez, Instituto de Ingeniería y Tecnología, Juárez, México

<sup>2</sup>Universidad Autónoma de Coahuila, Facultad de Ciencias Químicas, Saltillo, México

## Corresponding author:

Imelda Olivas-Armendáriz, Departamento de Física y Matemáticas, Instituto de Ingeniería y Tecnología, Universidad Autónoma de Ciudad Juárez, Av. Del Charro No. 450 Norte, Col. Partido Romero, Ciudad Juárez C.P. Chihuahua 32320, México.

Email: [iolivas@uacj.mx](mailto:iolivas@uacj.mx)

skin, bone, muscle membrane, and tendon. Gelatin is considered a high molecular weight protein, integrated with 18 varieties of amino acids. This polymer has several biomedical applications, among which wound dressings stand out.<sup>5</sup> The compatibility between gelatin and CMC is due to the ability to link through electrostatic interactions. This compatibility occurs when CMC has various positive charges, and gelatin has various negative charges on their chains at appropriate pH conditions.<sup>6</sup>

Gelatin and CMC polymers can be used as components in the elaboration of wound dressing and regenerative biomaterials. Individually, CMC polymer has been extensively used in biomaterials technology as wound dressings due to its biodegradability, biocompatibility, non-toxicity, regenerative activity on tissues, tissue granulation promotion, and cicatrization acceleration.<sup>3</sup> Meanwhile, gelatin polymer is a proteinaceous biopolymer exhibiting properties like biodegradability, biocompatibility, water absorption, and easiness of chemical structure modification.<sup>7</sup>

The HA is used as a biomaterial due to its resemblance to the composition of most hard tissue of mammalian animals. Sometimes, it is employed as a coating layer for metallic substrates. HA's crystals have a composition of calcium (Ca), phosphor (P), and trace amounts of  $Mg^{2+}$ ,  $Zn^{2+}$ ,  $Sr^{2+}$ ,  $Ag^+$ ,  $Cl^-$  and  $F^-$  ions. Although HA is an osteoconductive and biocompatible material, it has limited antibacterial resistance. To overcome this problem, metallic ions have been added to HA structure, for example,  $Ag^+$  due it has strong bacterial growth inhibition properties.<sup>8</sup>

$Ag^+$  is used as toxic material for some bacteria cells, thus is widely added to different biomaterials to increase its antibacterial activity. HA doped with  $Ag^+$  has been obtained by several methods such as sintering, precipitation, microwave refluxing, ultrasonic precipitation electrostatic spray-pyrolysis, and sol-gel. Besides,  $Cu^+$  have mechanisms of antimicrobial activity, among which stand cell membrane disruption, DNA rupture and, production of reactive oxide species.<sup>9-11</sup> The aim of the present study is to develop a composite film of hydroxyapatite with ionic substitutions ( $Ag$  and  $Cu$ ) embedded into a polymer matrix to evaluate the antibacterial, bioactivity, and biocompatibility properties.

## Materials and methods

Composite films were prepared by mixing the OCMC, gelatin, and  $Ag-Cu/HA$  complex. Characterization of the chemical, thermal, morphological, degradability, hydrophobicity, antibacterial activity, and biocompatibility of the composite films was done in all prepared samples. The materials used during the experiments were: chitosan (75%–85% deacetylation, Medium Molecular Weight, Sigma-Aldrich), isopropanol (Sigma-Aldrich), NaOH (J.K. Pellets Baker), mono-chloroacetic acid (99%, Sigma-Aldrich), acetic acid (99%; Sigma-Aldrich), Gelatin (Sigma-Aldrich),

genipin (WM 226.2 g/mol, Challenge Bioproducts Co), glycerin (99%, Sigma-Aldrich), *Escherichia coli* (*E. coli*) (ATCC® 11,229™), *Staphylococcus aureus* (*S. aureus*) (ATCC® 6538™), lysozyme (Fisher Scientific), DMEM (1X, gibco), Fetal Bovine Serum (FBS) (Corning), Penicillin Streptomycin (gibco).

## Silver-Copper/hydroxyapatite complex

$Cu$  and  $Ag$  in concentrations of 0.1, 0.5, and 1.0 mol were used to prepare the  $Ag-Cu/HA$  complex. The  $Ag-Cu/HA$  composite was synthesized by the Martínez-Gracida method.<sup>12</sup> For the  $Ag-HA$  synthesis, citric acid was dissolved in deionized water, then  $Ca(NO_3)_2 \cdot 4H_2O$  and  $NH_4H_2PO_4$  were added. A homogeneous solution was obtained and, ethylene glycol was added at 70°C. The product was dried in an oven at 120°C for 12 h, and the recovered product was calcined at 1100°C for 2 h. On the other hand, for  $Cu-HA$  synthesis  $Ca(NO_3)_2 \cdot 4H_2O$  and  $(NH_4H_2PO_4 + CuSO_4 \cdot 5H_2O)$  were separately dissolved at a ratio of 1 g/50 mL in deionized water. Then, 40 mL of  $NH_4OH$  for each gram of  $NH_4H_2PO_4$  were added to the phosphate-copper solution and the temperature was increased to 75°C during 3h. The product was filtered, washed with deionized water, and dried at 90°C for 24 h. Then, it was treated at 500°C for 2 h. The materials were mixed with the help of a planetary mill at 250 r/min for 10 min at a ratio of 1:15 loads/balls. The mixes of the concentrations of  $Cu$  and  $Ag$  were prepared according to Table 1.

## Synthesis of OCMC

The synthesis of OCMC polymer was done through a carboxymethylation reaction. 5 grams of chitosan (75%–85% deacetylation, Sigma-Aldrich) were mixed with 50 mL of isopropanol (Sigma-Aldrich) for 2 h at room temperature under constant stirring. After this time, a 15 mL solution of sodium hydroxide NaOH (J.K. Pellets Baker) at 40% w/v was added and stirred constantly to deprotonate the hydroxyl groups (OH) of the chitosan chain. Subsequently, 100 mL of mono-chloroacetic acid (99%, Sigma-Aldrich) solution (25.5 g in 100 mL of isopropanol) was prepared, divided into 5 equal parts, and added every minute into the mix at room temperature and constant stirring. The carboxymethylation reaction was continued under constants stirring for 24 h at room temperature. After the reaction time elapsed, it was stopped by a wash with 70% of ethanol (99.6%; J.T. Baker) to remove salts and water. The pH of the obtained OCMC was adjusted to 7.4 with a 2% acetic acid (99%; Sigma-Aldrich) solution. Finally, the OCMC was dried under vacuum.<sup>13</sup>

## Composite films preparation

The composite films were prepared by a casting technique. Each solution was prepared with 2% w/v of OCMC and

**Table 1.** Au and Cu combinations.

Code	Concentration (mol)
C1	Ag 1.0 - Cu 1.0
C2	Ag 1.0 - Cu 0.5
C3	Ag 1.0 - Cu 0.1
C4	Ag 0.5 - Cu 1.0
C5	Ag 0.5 - Cu 0.5
C6	Ag 0.5 - Cu 0.1
C7	Ag 0.1 - Cu 1.0
C8	Ag 0.1 - Cu 0.5
C9	Ag 0.1 - Cu 0.1

Gelatin (Sigma-Aldrich) in 100 mL of distilled water under agitation for 10 min approximately. Then 0.1% w/w of genipin with respect to the polymer solution was added. Finally, 1 mL of glycerin was also added to the solution. For the films with Ag-Cu/HA complex, 0.005 g of the complex powder were added to each sample and mixed for 10 min. In 10 cm diameter plastic Petri dishes, 25 mL of each final solution were added. Finally, the solutions were evaporated at room temperature until the films were obtained (Figure 1). In total, nine composite films were made with different Ag-Cu/HA complex and a control film without complex. Another film with OCMC and gelatin 2% w/w was made without Ag-Cu/HA complex to have a control sample for all assays.

#### Fourier transform infrared spectroscopy (FT-IR)

The chemical composition analysis by FT-IR was used to assess the interactions between the materials in the composite films. The analysis was performed on a spectrophotometer (Nicolet 6700) in the region of 500–3000  $\text{cm}^{-1}$ , with a resolution of 16  $\text{cm}^{-1}$ .

#### Surface analysis: Morphology

The surface analysis of the composite films was performed by Scanning Electron Microscopy (SEM) (Hitachi model SU5000). The films were placed on double-sided adhesive tape. The images were captured using low vacuum an accelerating voltage of 15 kV. The embedded particles were measured using the image J analysis software and the reported values are the results of at least 100 measurements in more than three different images per condition.

#### Hydrophobicity study: Contact angle

The hydrophilicity of the surface of the films was studied by measuring the contact angle of a drop of distilled water at room temperature, using a goniometer (DSA 30, Kruss) and samples of 1  $\text{cm}^2$ . The contact angle was measured by the

goniometer's software and the percentage value was calculated by the average of three measurements on each film.

#### Thermal properties

The thermal properties of the composite films were determined by using a thermal analyzer, TGA (SDT Q600 TA instrument), with a temperature range at 25°C–600°C with a ramp of 10°/min in a nitrogen atmosphere.

#### Antibacterial activity

The antibacterial activity of the composite films was evaluated by the turbidimetry technique. Solutions containing *Escherichia coli* (*E. coli*) (ATCC® 11,229™), and *Staphylococcus aureus* (*S. aureus*) (ATCC® 6538™) were used as standard Gram-negative and Gram-positive bacteria respectively. Composite and control films of 1  $\text{cm}^2$  were used on the test. The films were put in 2 mL of each bacterial standard solution and incubated at 37°C (Thermo scientific, series 8000VW). After 1 day of incubation, the resulting solutions were measured by UV-visible light spectroscopy (Genesys 2, ThermoSpectronic) at a wavelength of 450 nm. The following equation was used to determine the percentage of antibacterial activity (AA%)

$$\text{AA\%} = \frac{\text{MF}_f - \text{AM}_i}{\text{AM}_f} \times 100\%$$

where:

AA% = percentage of antibacterial activity

AM<sub>f</sub> = Final absorbance measurement of the solution at 450 nm

AM<sub>i</sub> = Initial absorbance measurement of the solution at 450 nm

#### Enzymatic degradation assay

For each film, samples of 1  $\text{cm}^2$  were cut and weighted before adding in 1X PBS solution with a 7.4 pH. The in vitro enzymatic degradation was performed in tubes with 5 mL of 1X PBS solution with 0.02% Sodium azide (NaN<sub>3</sub>) and 5  $\mu\text{g}/\text{mL}$  lysozyme (Fisher Scientific) in incubation periods of 1, 2, and 3 days at 37°C without change of PBS solution. Then, each film sample was washed with distilled water and dried at room temperature. Subsequently, the weight loss percentage was calculated using the following equation

$$\text{WL\%} = \frac{W_i - W_f}{W_i} \times 100\%$$

where:

WL% = weight loss percentage

W<sub>f</sub> = final weight

W<sub>i</sub> = initial weight

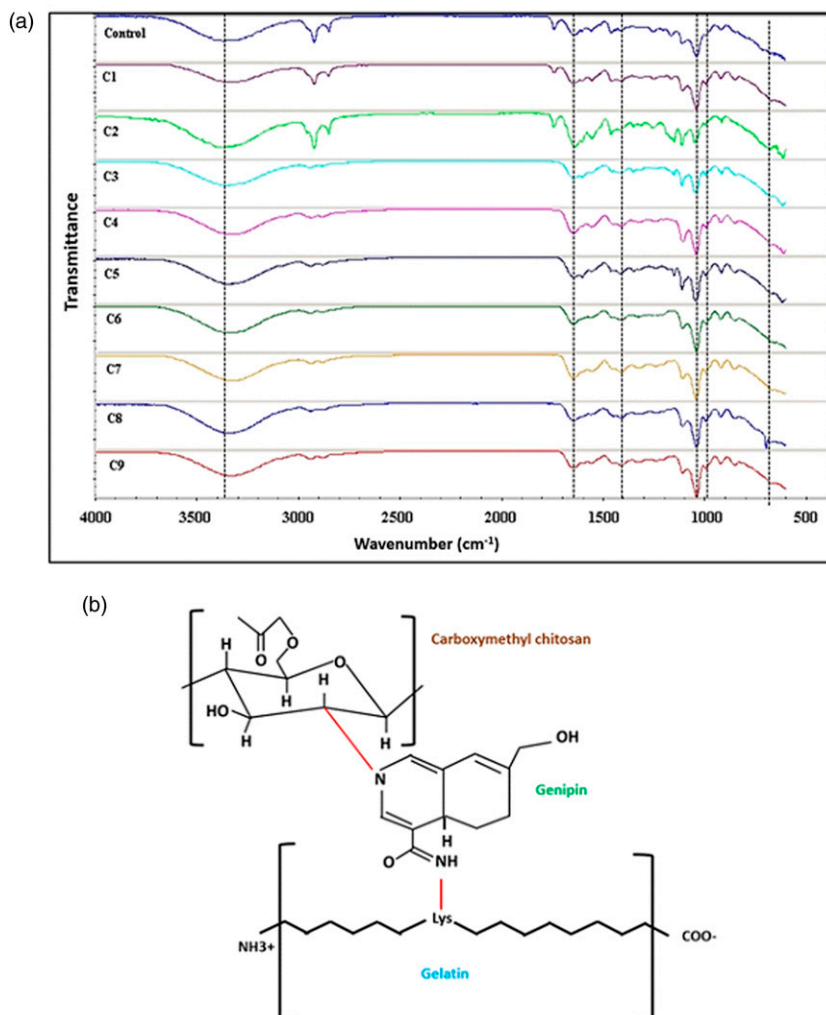


**Figure 1.** (a) FT-IR spectra of composite films and (b) Carboxymethyl chitosan/Gelatin crosslinked with genipin representation.

After the samples were weighed, they were analyzed by SEM to observe the degree of degradation of the surface films. An energy dispersion system (EDS) was used to analyze the presence of Cu-Ag- Ha complex particles in the surface after being exposed to the enzymatic PBS solution during different periods of time. Finally, the pH of the PBS solution obtained from the degradation was determined.

### Cell morphology and viability

Embryonic cell line 3T3 murine fibroblasts (ATCC) was used in this analysis. Composite films were cut into 1 cm<sup>2</sup> and sterilized by UV light in a laminar flow cabinet (Labconco, logic Type A2). Then, 50,000 fibroblasts were seeded with DMEM (1X, gibco) supplement with 10% FBS (Corning) and 1% Penicillin- Streptomycin (gibco) on each

sample and incubated at 37°C in 5% CO<sub>2</sub> during 24 and 72 h. Cells viability analysis was realized by the tetrazolium colorimetric MTT assay.

To evaluate the adhesion and morphology cell, 50,000 fibroblasts were seeded with 3 mL of DMEM supplement on each sample in 24-well plates. All 24-well plates were incubated at 37°C with 5% CO<sub>2</sub> for 24 and 72 h. The cell adhesion and morphology of the seeded fibroblasts were observed by optical microscopy (Zeiss Axio Vert. A1) at 40X by the hematoxylin-eosin stain.

### Statistical analyses

The values were expressed on the results have means ± standard deviation. Whenever appropriate, T Student's test was used to discern the statistical differences between film results. A *p* value of less than 0.05 was statistically significant.

## Results and discussion

### Chemical composition analysis

The IR spectroscopic analysis provided the chemical information of the composite films (Figure 1(a)). The infrared spectra show that the films were distinguished by the presence of amide bond peak  $\sim 1656\text{--}1644\text{ cm}^{-1}$  (N-H deformation), and a peak  $\sim 1560\text{--}1335\text{ cm}^{-1}$  corresponding to C=O stretching of the gelatin. The presence of OCMC on the film was determined by peaks at  $\sim 1320\text{ cm}^{-1}$  (C-H stretch),  $\sim 1150\text{ cm}^{-1}$  (bridge O stretch),  $\sim 1080\text{ cm}^{-1}$  (C-O stretch),  $\sim 1600\text{ cm}^{-1}$  (N-H bending),  $\sim 1640\text{ cm}^{-1}$  (C-N Schiff's base), and  $1400\text{ cm}^{-1}$  corresponding to  $-\text{CH}_2\text{-COOH}$  group.  $3350\text{ cm}^{-1}$  peak corresponds to the O-H stretching. The increased intensity of this peak in  $3350\text{ cm}^{-1}$  suggests an increased intermolecular hydrogen bonding. Various research has found significant interactions at the molecular level between gelatin and OCMC polymer structures (Figure 1(b)), which are generated by electrostatic interactions.<sup>14</sup>

The intensity of the peak near  $3400\text{ cm}^{-1}$  in the control film suggests increased intermolecular hydrogen bonding between gelatin and OCMC.<sup>15</sup> Specifically, the control film had an increase between the intensities for the adsorption band at  $1600$  to  $1640$  and  $1550$  to  $1589\text{ cm}^{-1}$ , where according to others researches it is explained by the amide C=O and amines N-H bonds between gelatin macromolecules and OCMC by crosslinking with the Genipin molecule.<sup>16</sup> On the other hand, the addition of Ag-Cu/HA does not have the ability of direct reinforcement due to the lack of chemical interactions with the polymer. However, it is distributed within the polymeric matrix in low amounts as seen in the peaks at  $602\text{ cm}^{-1}$  and  $650\text{ cm}^{-1}$  that correspond to vibrations of  $\text{PO}_4^{3-}$ , suggesting an interaction between the polymer matrix.<sup>17</sup> Also, the peak around at  $1080\text{--}1050\text{ cm}^{-1}$  and  $700\text{--}600\text{ cm}^{-1}$  in some composite films corresponded to the  $\text{PO}_4^{3-}$  and  $\text{HPO}_4^{2-}$  vibrations, respectively, and the superposition of the -OH groups and amide II groups between HA and polymer matrix.<sup>18</sup>

### Surface morphology

Figure 2 shows secondary electron images obtained by SEM of the surfaces of all films. In general, it is seen that the crosslinking of gelatin with OCMC provides smooth surfaces to the films (Figure 2(a)), both polymers tend to give that property to the copolymers in which they are used. Ag-Cu/HA complex when mixed with the rest of the compounds at the time of synthesis, and not sprayed or dusted on the surface, appears as embedded particles of irregular morphology in the range size of approximately  $2\text{--}47\text{ }\mu\text{m}$ . The incorporation of Ag-Cu/HA complex into the polymer matrix provides certain roughness to its surface (Figure 2 from b to j).

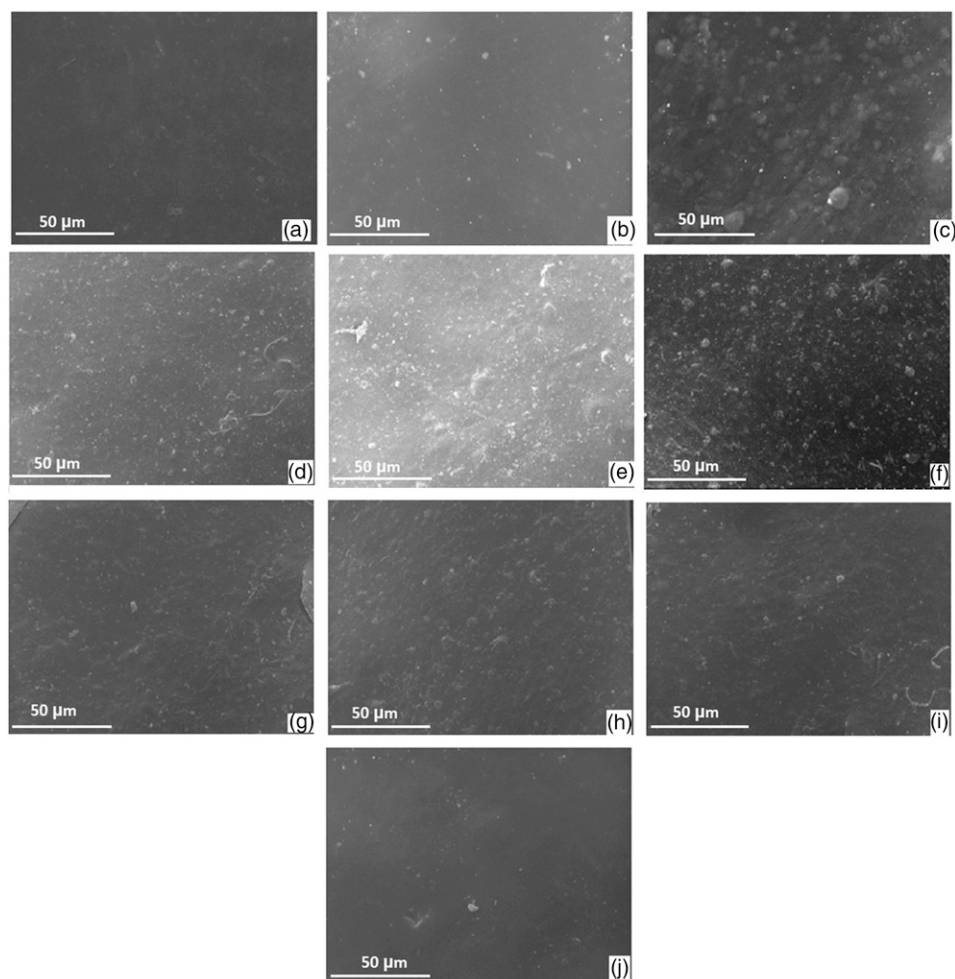
### Composite films thermal stability

Figure 3 shows the TGA curve of the different composite films. As a general trend, it is observed that the films with the Ag-Cu/HA complex exhibit greater thermal stability compared to the control film, this is due to the good stability of HA ends and the interaction of HA with both polymers, which can be explained by the increase of additional OH groups by the chemical structure of HA, which leads to an increase in the hydrogen bridge bonds between the components of the films.<sup>19</sup> The addition of Cu and Ag particles in the films also helps to reduce the weight loss of the films at the end of the test. On the other hand, samples C6 and C9 display greater weight loss compared to the control film in the early stages of the test; these films have a lower concentration of Ag and Cu.

The results suggest that the addition of Ag-Cu/HA complex enhances the thermal stability of films. Thermal stability analysis in biomaterials is essential not only at the temperature limits of the human body but also at a higher temperature range for post-manufacturing processes such as the thermal sterilization processes. In all the films there is a lower weight loss, between 3 and 4.55%, below  $126.17^\circ\text{C}$  (Step I), corresponding to the removal of the water associated with the OH of the polymers and the water. A significant weight loss is seen between  $126$  and  $395^\circ\text{C}$  (Step II), it is attributed to the decomposition of polymers, in the case of gelatin it has a decomposition temperature of between  $250$  to  $400^\circ\text{C}$ .<sup>14</sup> The decomposition of OCMC is between temperatures of  $160\text{--}530^\circ\text{C}$  due in great part to the volatilization of small molecules and the formation of carbonized products of the polymer. When the films have 50% degradation, the temperatures reached are in the range from  $190$  to  $225^\circ\text{C}$ .<sup>20</sup> Finally, in step III a loss between 25 and 45% is observed, this loss corresponds to thermal decomposition with depolymerization at higher temperatures up to  $600^\circ\text{C}$ , as shown in Table 2.

### Contact angle measure

This characterization is used to analyze the possible interactions between the surface of the biomaterial and the cells. The hydrophilic character of any substance or material is based on the quantity of strong polar groups on its polymer structure, which facilitate interplay with water molecules. The contact angle values obtained on the films are shown in Table 3, where CA (A) is the average of the contact angle, CA (L) is the left side contact angle and CA (R) is the contact angle of the right side of the drop. Figure 4 shows the images obtained during the measurement of angles CA [L] and CA [R]. The incorporation of a carboxymethyl group into the main chain of chitosan causes an increase in the hydrophilic character of the material. In general, CA (A) showed a significant variation in all films.



**Figure 2.** SEM images of (a) control film, (b) C1 film, (c) C2 film, (d) C3 film, (e) C4 film, (f) C5 film, (g) C6 film, (h) C7 film, (i) C8 film and, (j) C9 film.

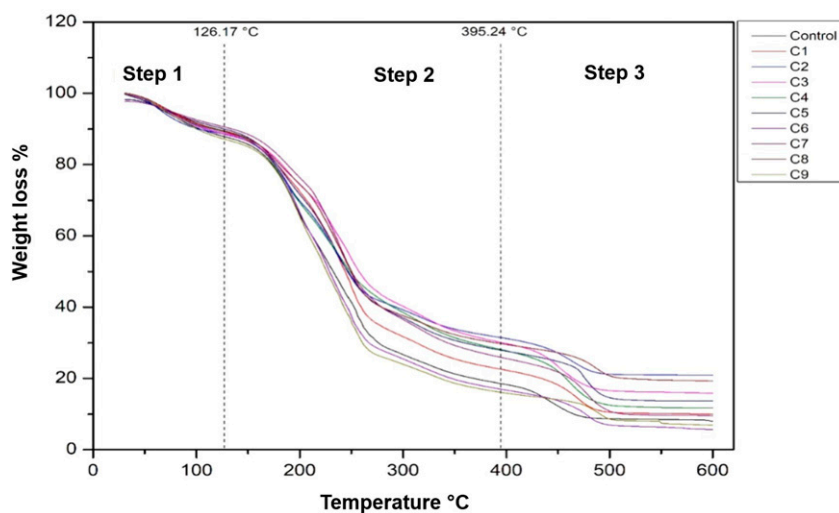


**Figure 3.** TGA pattern of the composite films.

**Table 2.** Composite films thermal stability results.

Sample/Weight loss	Step I (30–126.17°C) (%)	Step II (126.17–394.24°C) (%)	Step III (394.24°C–600°C) (%)	Residual mass (%)
Control	3.09	58.51	30.41	7.99
C1	3.81	50.17	36.03	9.99
C2	4.07	38.59	36.46	20.88
C3	3.8	41.67	38.71	15.82
C4	4.32	41.74	42.23	11.71
C5	3.42	39.74	43.34	13.50
C6	4.14	58.01	32.17	5.68
C7	3.04	37.69	49.74	9.53
C8	4.55	42.71	33.45	19.29
C9	3.98	58.84	30.31	6.87

**Table 3.** Contact angle results.

Film	CA (A)	CA [L]	CA [R]
<b>Control</b>	71.4	71.5	71.3
<b>C1</b>	81.25	80.8	81.7
<b>C2</b>	70.65	70.2	71.1
<b>C3</b>	72.65	76	69.3
<b>C4</b>	71.25	70.7	71.8
<b>C5</b>	83.5	78.4	88.6
<b>C6</b>	73.25	77.7	68.8
<b>C7</b>	83.15	88	78.3
<b>C8</b>	74.3	72.3	76.3
<b>C9</b>	70.9	70.1	71.7

Only C1, C5, and C8 films exhibited contact angles of 81.25%, 83.5%, and 83.15% respectively, a significant increase in CA (A) compared to the control film with 71.4%, which can be attributed to a higher concentration of Cu in the Ag-Cu/HA complex used in the manufacture of composite films. Previous researchers have shown that the incorporation of Cu and Zn ions into chitosan and nano-HA biomaterials significantly increases swelling, and thus the interaction with water molecules.<sup>8</sup> On the other hand, the water absorption property establishes the diffusivity of the nutrients from the biomaterial matrix. Also, this property averts the accumulation of fluid exudates produced at the wound site.<sup>15</sup> It is important to analyze the contact angle of biomaterials to study the surface free energy values and their polar components. The contact angle in polymers is mainly associated with the swelling of the polymeric matrix and the hygroscopic character of the material's surface. Due to the positive charges of its molecules, the chain of the chitosan interacts with cell membranes through electrostatic forces, a useful property in various biomedical applications.<sup>21</sup> The incorporated the carboxymethyl molecule (CH<sub>2</sub>COOH) on the chitosan chain, the composite films elaborated with OCMC acquire a greater hydrophilic character than those made with their precursor.

### Enzymatic degradation

Figure 5(c) show the secondary electron images and elemental analysis by EDS of the film C1 exposed in PBS containing lysozyme enzyme at different periods, as an example of the degradation process of the composite films. During the first 24 h (Figure 5(c1)), the image shows a homogeneous surface due to the polymeric matrix of O-CMC/gelatin since the elemental analysis shows characteristic elements of these materials such as carbon, nitrogen, oxygen, while elements such as sodium and chlorine can be attributed to scraps of 1X PBS solution after the biodegradability test. It should be noted that after 48 h (Figure 5(c2)) and 72 h (Figure 5(c3)) of exposure to the degradation solution, the morphology appears porous, confirming the degradation of the polymers, this can be attributed to the catalyzed hydrolysis of the lysozyme, it is also verified with the data reported in the weight loss percentage results. Finally, in the EDS of the sample at 2 and 3 days, an increase in phosphorus (P) and calcium (Ca) is observed, presenting elements in the HA composition. The weight loss results are shown in Figure 6(a) exhibit a gradual weight loss for the first 24 h to all films, with a loss of 55%, after 48 h of exposure with the lysozyme, a maximum weight loss between 65% and 78.63% was seen at 72 h of exposition. Considering the interaction of the lysozyme and the polymer matrix, since O-CMQ is a polysaccharide, it is degraded by enzymatic hydrolysis.<sup>13</sup>

In other studies, in scaffolds made with gelatin, chitosan, and hydroxyapatite, it was shown that the degradation increases with the incorporation of gelatin but decreases when the hydroxyapatite is added to the biomaterial,<sup>22</sup> a similar trend was observe in the composite films with Ag-Cu/HA, compared to the OCMC and gelatin control film. The changes in pH seen during the biodegradation period of the material were monitored during the 72h exposure of 1 X PBS with lysozyme (Figure 5(b)). The solution's

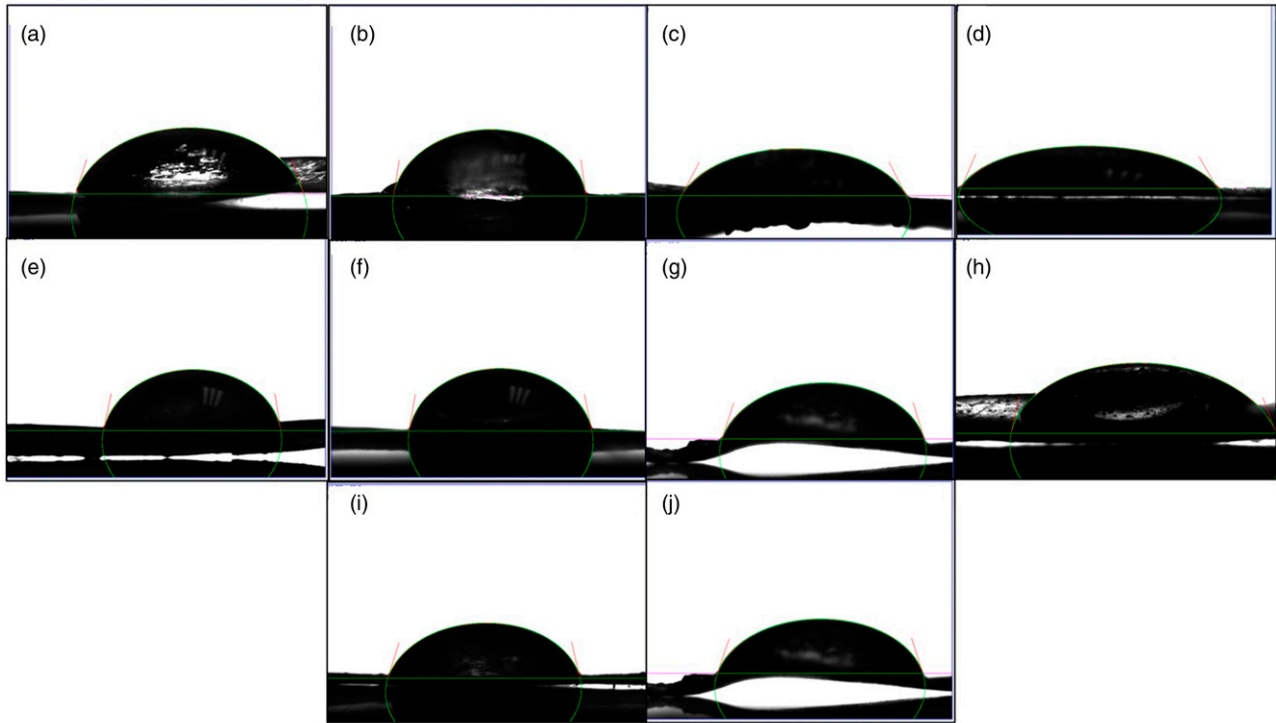


**Figure 4.** Contact angle measure if the film: (a) Control, (b) C1, (c) C2, (d) C3, (e) C4, (f) C5, (g) C6, (h) C7, (i) C8, and (j) C9.

pH fluctuated in a narrow range of 6.8–6.3. In the first 24 h of degradation, the pH decreased from 7.4 to the range of 6.7–6.5, which may be due to the degradation of the residual amino or acetic acid group of the composite material, since the variations were close to a neutral pH, it can be concluded that the dressing will not have adverse damage to the host.<sup>23</sup>

### Antimicrobial activity

Figure 6(a) shows the antibacterial activity test of the films against Gram-positive bacteria (*S. aureus*) and Gram-negative bacteria (*E. coli*) at 24 h of exposition. The control film obtained 49.3% and 40.50% antibacterial activity for gram-negative and gram-positive bacteria respectively, this activity may be due to OCMC polymer, which, as its precursor chitosan, has reported antimicrobial activity.<sup>3,13</sup> By adding Ag-Cu/HA complex to the films, the antibacterial activity increases compared to the control film, and this is because HA, Ag and Cu ions have a higher antimicrobial activity than OCMC.<sup>9,8,12</sup> However, films C1, C2, C3, and C4 obtained a significantly higher percentage of antibacterial activity than the other composite films, with percentages ranging from 72.5% to 82.4% for Gram-negative bacteria, and between 77.78% to 81.09% for Gram-positive bacteria. This suggests that the higher concentration of Ag in the Ag-Cu/HA complex increases the antibacterial activity of the film both bacteria.

All films were made with OCMC, which is a polymer with reported antibacterial activity.<sup>19</sup> The bactericidal activities of chitosan and its derivatives against *E. coli* increase which is due to the increment quantity of  $\text{NH}_3^+$  groups in the polymer chains. The substitution in OCMC only takes place at hydroxyl groups in the chain, thus the number of  $\text{NH}_3^+$  groups stay constant after carboxymethylation reaction, occasioning a major antibacterial activity for the OCMC polymer.<sup>3</sup> *S. aureus* is a bacterium that causes post-surgical wound infections. The antibacterial activity of HA is mainly attributed to  $\text{Ca}^{+2}$ . Some investigations have reported that  $\text{Ca}^{+2}$  ions are active membrane bactericide that destabilizes the cell membrane and kills the stationary phase of *S. aureus*. On the other hand, hydroxyl ions of HA produce a lethal effect on some bacterial cells.<sup>9</sup> Silver ion ( $\text{Ag}^+$ ) and copper ion ( $\text{Cu}^+$ ) are the most frequent dopants for HA. The Ag ion has an ample spectrum of antimicrobial activity, also, bacterial resistance is less likely to occur with its use.<sup>8</sup> Other research confirms that the incorporation of Cu in HA helps to increase the antimicrobial activity of the Cu/HA complex in different biomaterials.<sup>24</sup> For example, H. Yang, et al., investigated that the proliferation of *E. coli* and *Streptococcus mutans* bacteria on nanosized Ag/Cu-HA, this research showed the great antibacterial activity of the complex.<sup>25</sup> Other research found that a hydrogel film elaborated from CMC loaded with waterborne polyurethane-gelatin hydrolysate presented significant



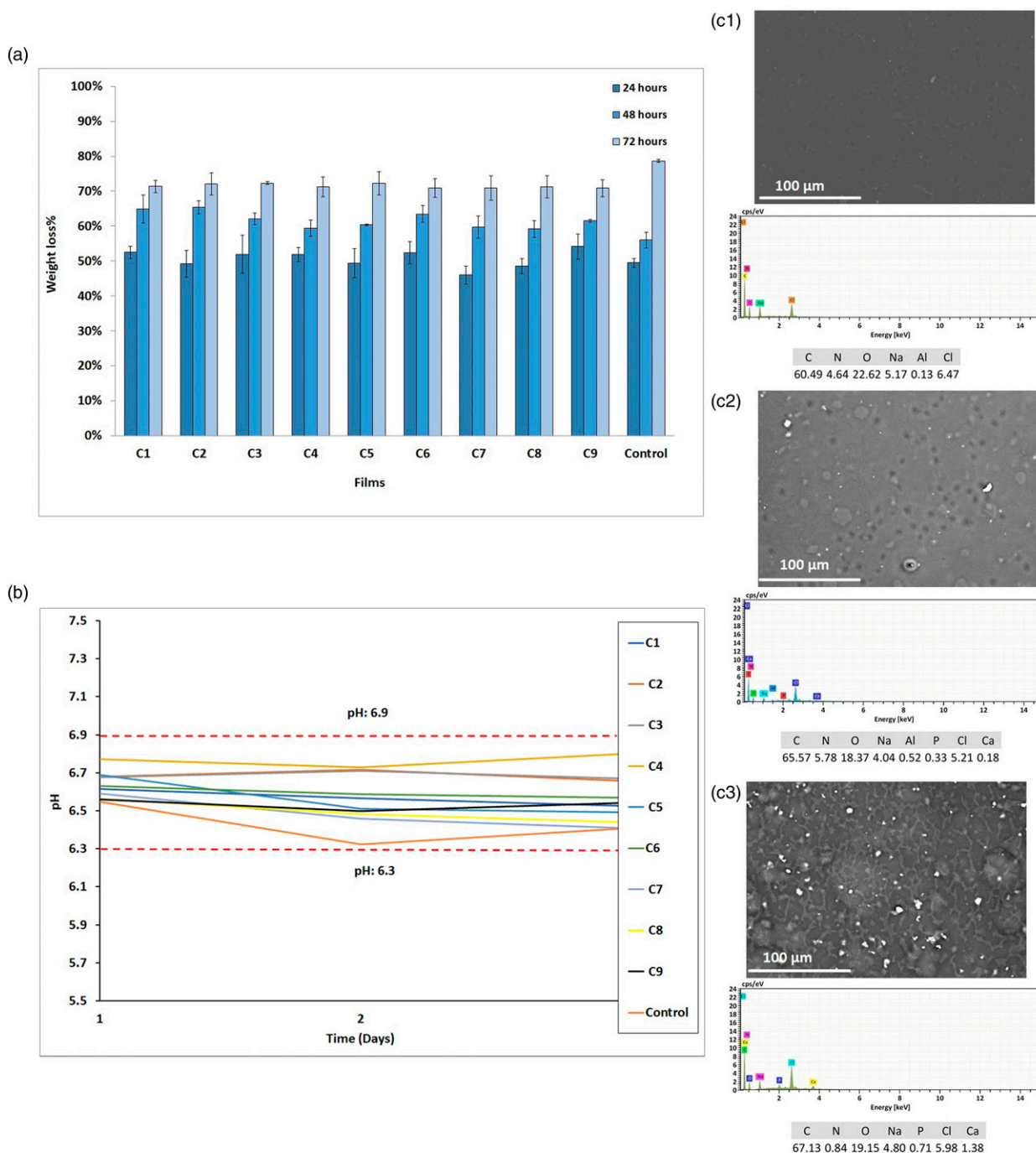


**Figure 5.** Degradation enzymatic results: (a) the weight loss percentage of de films during enzymatic degradation on 1, 2, and 3 days, data represent mean  $\pm$  S.D. ( $n = 5$ ), (b) pH variation of the PBA solution during enzymatic degradation on 1, 2 and 3 days, (c) Observation of the morphology and chemical composition of the surface by SEM-EDS of the C9 sample: (c1) day 1, (c2) day 2 and, (c3) day 3.

antibacterial activity against *E. coli* and *S. aureus*.<sup>26</sup> Also, OCMC hydrogels were prepared by Ag/AgO in situ precipitation method have an inhibition rate of *E. coli* reaching the maximum of 92.32%.<sup>27</sup>

**Fibroblast cell viability**

Figure 6(b) shows the percentage of cell viability of the materials seeded with fibroblasts. According to ISO

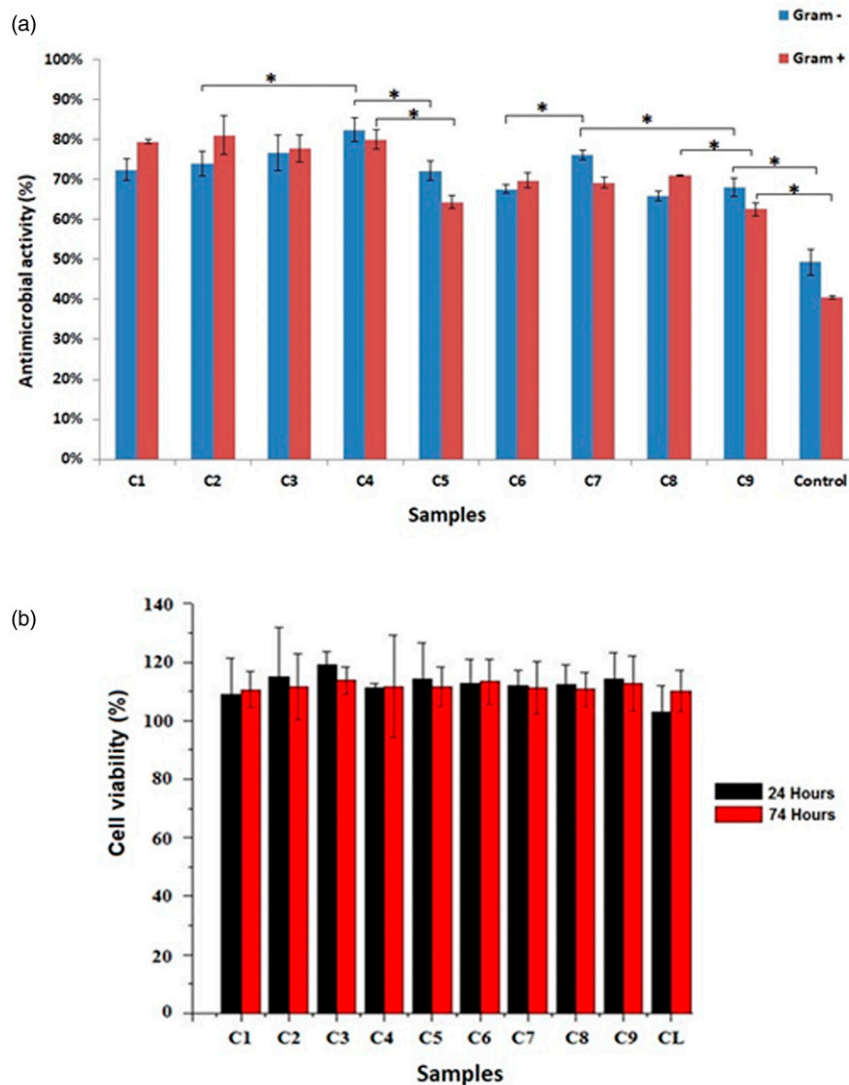


**Figure 6.** (a) Antibacterial properties films result on Gram<sup>-</sup> and Gram<sup>+</sup> bacteria at 24 h, (b) Cell viability percentage of fibroblasts seeded on the films at 24 and 72 h. Data represents mean  $\pm$  S.D. ( $n = 5$ ), \* $p < 0.05$ .

10,993-5:2009, Typically, if a biopolymer exhibits a viability percentage is greater than 70% the material is considered not potentially cytotoxic.<sup>28</sup> To corroborate that time is not a factor that affects the cytotoxicity of the material, analyzes were made at 24 and 72 h of culture, finding that in both periods the percentage of cell viability is above 80%, which suggests that the material obtained does not cause cellular damage. All samples containing the doped hydroxyapatite showed an increase in viability above 100%, suggesting that the incorporation of this compound helps cell proliferation during the test. However, there was no significant difference between composite films and the control film, suggesting that the incorporation of the Ag-Cu/HA complex does not significantly affect fibroblast cell viability and proliferation. Finally, a slight increase in proliferation

was observed at 72 h concerning the proliferation at 24 h in all films.

Figure 7 shows fibroblasts seeded in the films at 24 and 72 h of culture. Good adhesion of fibroblasts to the surface of the films and the control is observed at 24 h of culture, achieving a uniform and well-organized adherence on the surface of the material. An increase in proliferation was seen at 72 h, which suggests that the material could be good support for wound healing. A greater proliferation was seen in the composite films than in the control. The fibroblasts showed a normal morphology of elongated cells in the shape of a crescent, with an ovoid nucleus, the cytoplasm of pink color being perceived in all the samples, as well as the nucleus in dark purple color.

On the other hand, the surface roughness of the films with the incorporation of the conjunction with the presence of functional groups and the surface hydrophilicity of the

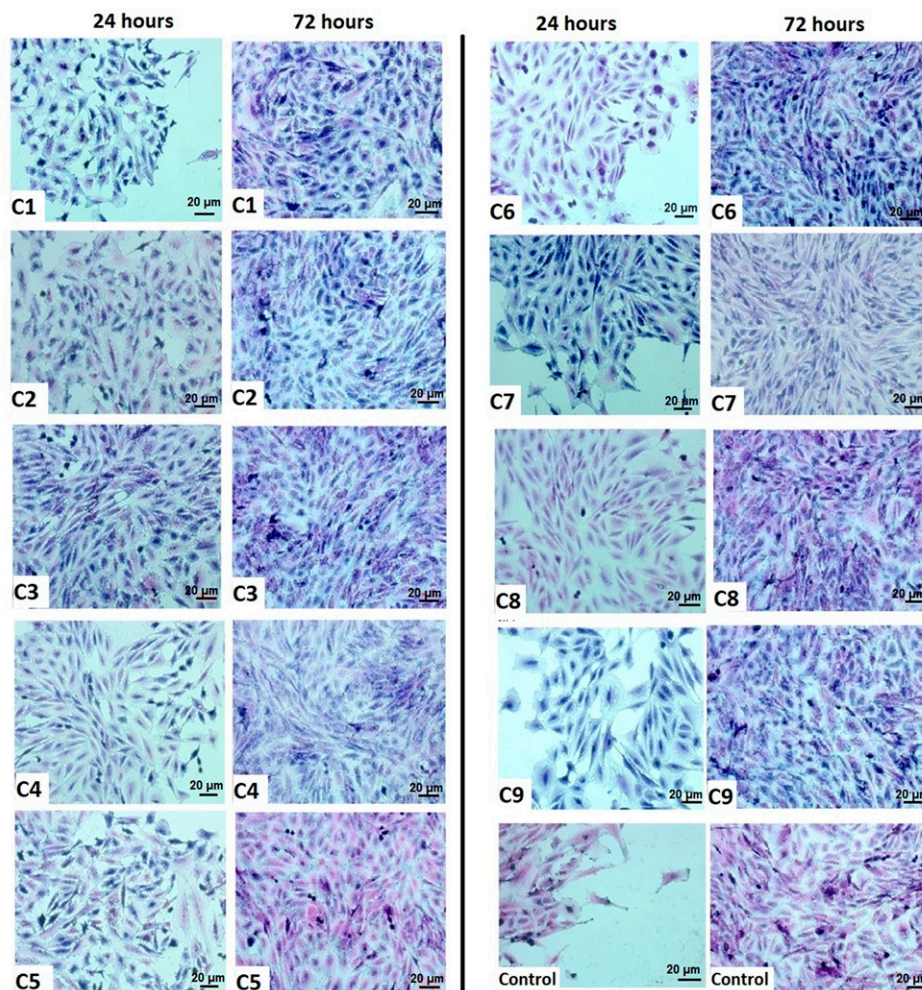


**Figure 7.** Images (40 × magnification) of fibroblasts seeded on the films after 24 and 72 h with hematoxylin and eosin staining.

polymeric matrix can help adhesion cells to the composite films.<sup>29</sup> These results are very important since dermal fibroblasts play a key role in the turnover of extracellular proteins in the skin, the interaction of the extracellular matrix, and cell-cell communication.<sup>30</sup> Research of Graphene-based HA composites exhibited great properties for tissue regeneration, like the adhesion, proliferation, and differentiation of osteoblasts and fibroblasts cells.<sup>31</sup>

## Conclusions

The structures of OCMC and gelatin, as well as their crosslinking through the genipin molecule, allowed not only their interaction through intermolecular forces but also their possible interaction with the Ag-Cu/HA complex. The inclusion of the Ag-Cu/HA complex and the intermolecular interactions between the different materials have also positive influence on the thermal, mechanical, surface topography, degradation and antibacterial properties of the composite films compared to the OCMC/gelatin film. Moreover, composite films showed cellular viabilities

greater than 100%. Results indicate that composite films can be used as a wound healing dressing and regenerating biomaterial.

## Declaration of conflicting interests

The author(s) declared no potential conflicts of interest with respect to the research, authorship, and/or publication of this article.

## Funding

The author(s) disclosed receipt of the following financial support for the research, authorship, and/or publication of this article: The authors acknowledge the financial support of the Mexican National Council for Science and Technology (CONACyT) through project SEP-CONACyT CB 2015-01-252439.

## ORCID iDs

Elia M Múzquiz-Ramos  <https://orcid.org/0000-0001-8626-678X>  
Imelda Olivas-Armendáriz  <https://orcid.org/0000-0003-2233-0310>

## References

1. Upadhyaya L, Singh J, Agarwal V, et al. Biomedical applications of carboxymethyl chitosans. *Carbohydr Polym* 2013; 91: 452–466. DOI: [10.1016/j.carbpol.2012.07.076](https://doi.org/10.1016/j.carbpol.2012.07.076).
2. Fonseca-Santos B, Chorilli M, et al. An overview of carboxymethyl derivatives of chitosan: Their use as biomaterials and drug delivery systems. *Mater Sci Eng C* 2017; 77: 1349–1362. DOI: [10.1016/j.msec.2017.03.198](https://doi.org/10.1016/j.msec.2017.03.198).
3. Shariatnia Z. Carboxymethyl chitosan: properties and biomedical applications. *Int J Biol Macromol* 2018; 120: 1406–1419. DOI: [10.1016/j.ijbiomac.2018.09.131](https://doi.org/10.1016/j.ijbiomac.2018.09.131).
4. Ruyu B, Xin Z, Huimin Y, et al. Development and characterization of antioxidant active packaging and intelligent Al<sup>3+</sup>-sensing films based on carboxymethyl chitosan and quercetin. *Int J Biol Macromol* 2019; 126: 1074–1084. DOI: [10.1016/j.ijbiomac.2018.12.264](https://doi.org/10.1016/j.ijbiomac.2018.12.264).
5. Liang M, Li Z, Gao C, et al. Preparation and characterization of gelatin/sericin/carboxymethyl chitosan medical tissue glue. *J Appl Biomater Funct* 2018; 16: 97–106. DOI: [10.5301/jabfm.5000384](https://doi.org/10.5301/jabfm.5000384).
6. Bonilla J, Poloni T, Lourenço RV, et al. Antioxidant potential of eugenol and ginger essential oils with gelatin/chitosan films. *Food Biosci* 2018; 23: 107–114. DOI: [10.1016/j.fbio.2018.03.007](https://doi.org/10.1016/j.fbio.2018.03.007).
7. Patel S, Srivastava S, Singh MR, et al. Preparation and optimization of chitosan-gelatin films for sustained delivery of lupeol for wound healing. *Int J Biol Macromol* 2018; 107: 1888–1897. DOI: [10.1016/j.ijbiomac.2017.10.056](https://doi.org/10.1016/j.ijbiomac.2017.10.056).
8. Yilmaz B, Alshemary AZ and Evis Z. Co-doped hydroxyapatites as potential materials for biomedical applications. *Microchem J* 2019; 144: 443–453. DOI: [10.1016/j.microc.2018.10.007](https://doi.org/10.1016/j.microc.2018.10.007).
9. Riaz M, Zia R, Ijaz A, et al. Synthesis of monophasic Ag doped hydroxyapatite and evaluation of antibacterial activity. *Mater Sci Eng C* 2018; 90: 308–313. DOI: [10.1016/j.msec.2018.04.076](https://doi.org/10.1016/j.msec.2018.04.076).
10. Niu X, Wei Y, Liu Q, et al. Huang Silver-loaded microspheres reinforced chitosan scaffolds for skin tissue engineering. *Eur Polym J* 2020; 134: 109861. DOI: [10.1016/j.eurpolymj.2020.109861](https://doi.org/10.1016/j.eurpolymj.2020.109861).
11. Godoy-Gallardo M, Eckhard U, Delgado LM, et al. Antibacterial approaches in tissue engineering using metal ions and nanoparticles: From mechanisms to applications. *Bioact Mater* 2021; 6: 4470–4490. DOI: [10.1016/j.bioactmat.2021.04.033](https://doi.org/10.1016/j.bioactmat.2021.04.033).
12. Martínez-Gracida NO, Esparza-González SC, Castillo-Martínez NA, et al. Synergism in novel silver-copper/hydroxyapatite composites for increased antibacterial activity and biocompatibility. *Ceram Int* 2020; 46: 20215–20225. DOI: [10.1016/j.ceramint.2020.05.102](https://doi.org/10.1016/j.ceramint.2020.05.102).
13. Valencia-Gómez LE, Martel-Estrada SA, Vargas-Requena CL, et al. Characterization and evaluation of a novel O-carboxymethyl chitosan films with Mimosa tenuiflora extract for skin regeneration and wound healing. *J Bioact Compat Polym* 2020; 35: 39–56. DOI: [10.1177/0883911519885976](https://doi.org/10.1177/0883911519885976).
14. Qiao C, Ma X, Zhang J, et al. Molecular interactions in gelatin/chitosan composite films. *Food Chem* 2017; 235: 45–50. DOI: [10.1016/j.foodchem.2017.05.045](https://doi.org/10.1016/j.foodchem.2017.05.045).
15. Agarwal T, Narayan R, Maji S, et al. Gelatin/Carboxymethyl chitosan based scaffolds for dermal tissue engineering applications. *Int J Biol Macromol* 2016; 93: 1499–1506. DOI: [10.1016/j.ijbiomac.2016.04.028](https://doi.org/10.1016/j.ijbiomac.2016.04.028).
16. Chiono V, Pulieri E, Vozzi G, et al. G. Genipin-crosslinked chitosan/gelatin blends for biomedical applications. *J Mater Sci Mater Med* 2017; 19: 889–898. DOI: [10.1007/s10856-007-3212-5](https://doi.org/10.1007/s10856-007-3212-5).
17. Dumont VC, Mansur AAP, Carvalho SM, et al. Chitosan and carboxymethyl-chitosan capping ligands: Effects on the nucleation and growth of hydroxyapatite nanoparticles for producing biocomposite membranes. *Mater Sci Eng C* 2016; 59: 265–277. DOI: [10.1016/j.msec.2015.10.018](https://doi.org/10.1016/j.msec.2015.10.018).
18. Vo TS, Vo TTBC, Nguyen TS, et al. Incorporation of hydroxyapatite in crosslinked gelatin/chitosan/poly(vinylalcohol) hybrids utilizing as reinforced composite sponges, and their water absorption ability. *Prog Nat Sci Mater* 2021; 31: 664–671. DOI: [10.1016/j.pnsc.2021.09.003](https://doi.org/10.1016/j.pnsc.2021.09.003).
19. Mohamed NA, Mohamed RR and Seoudi RS. Synthesis and characterization of some novel antimicrobial thiosemicarbazone O-carboxymethyl chitosan derivatives. *Int J Biol Macromol* 2014; 63: 163–169. DOI: [10.1016/j.ijbiomac.2013.10.044](https://doi.org/10.1016/j.ijbiomac.2013.10.044).
20. Zhao M, Zhou H, Chen L, et al. Carboxymethyl chitosan grafted trisiloxane surfactant nanoparticles with pH sensitivity for sustained release of pesticide. *Carbohydr Polym* 2020; 243: 116433. DOI: [10.1016/j.carbpol.2020.116433](https://doi.org/10.1016/j.carbpol.2020.116433).
21. Wiącek AE, Terpiłowski K, Jurak M, et al. Effect of low-temperature plasma on chitosan-coated PEEK polymer characteristics. *Eur Polym J* 2016; 78: 1–13. DOI: [10.1016/j.eurpolymj.2016.02.024](https://doi.org/10.1016/j.eurpolymj.2016.02.024).
22. Yadav N and Srivastava P. In vitro studies on gelatin/hydroxyapatite composite modified with osteoblast for bone bioengineering. *Heliyon* 2019; 5(5): e01633. DOI: [10.1016/j.heliyon.2019.e01633](https://doi.org/10.1016/j.heliyon.2019.e01633).
23. Mobika J, Rajkumar M, Nithya Priya V, et al. Effect of chitosan reinforcement on properties of hydroxyapatite/silk fibroin composite for biomedical application. *Phys E: Low-Dimens. Syst Nanostructures* 2021; 131: 114734. DOI: [10.1016/j.physe.2021.114734](https://doi.org/10.1016/j.physe.2021.114734).
24. Rivera LR, Cochis A, Biser S, et al. Antibacterial, pro-angiogenic and pro-osteointegrative zein-bioactive glass/copper based coatings for implantable stainless steel aimed at bone healing. *Bioact Mater* 2021; 6: 1479–1490. DOI: [10.1016/j.bioactmat.2020.11.001](https://doi.org/10.1016/j.bioactmat.2020.11.001).
25. Yang H, Zhang L and Xu kw. Effect of storing on the microstructure of Ag/Cu/HA powder. *Ceram Int* 2009; 35: 1595–1601. DOI: [10.1016/j.ceramint.2008.09.012](https://doi.org/10.1016/j.ceramint.2008.09.012).
26. Zhang M, Yang M, Woo MW, et al. High-mechanical strength carboxymethyl chitosan-based hydrogel film for antibacterial

- wound dressing. *Carbohydr Polym* 2021; 256: 117590. DOI: [10.1016/j.carbpol.2020.117590](https://doi.org/10.1016/j.carbpol.2020.117590).
27. Yanqin X, Jie L, Shumin G, et al. A novel Ag/AgO/carboxymethyl chitosan bacteriostatic hydrogel for drug delivery. *Mater Res Express* 2020; 7: 8. DOI: [10.1088/2053-1591/aba5cd](https://doi.org/10.1088/2053-1591/aba5cd).
  28. ISO 10993-5:2009. Biological evaluation of medical devices — Part 5: Tests for in vitro cytotoxicity. ICS: 11.100.20 Biological evaluation of medical devices.
  29. Krishnan R, Rajeswari R., Venugopal J, et al. Polysaccharide nanofibrous scaffolds as a model for in vitro skin tissue regeneration. *J Mater Sci Mater Med* 2012; 23: 1511–1519. DOI: [10.1007/s10856-012-4630-6](https://doi.org/10.1007/s10856-012-4630-6).
  30. Lerman OZ, Galiano RD, Armour M, et al. Cellular dysfunction in the diabetic fibroblast: impairment in migration, vascular endothelial growth factor production, and response to hypoxia. *Am J Pathol* 2003; 162: 303–312. DOI: [10.1016/s0002-9440\(10\)63821-7](https://doi.org/10.1016/s0002-9440(10)63821-7).
  31. Li M, Xiong P, Yan F, et al. An overview of graphene-based hydroxyapatite composites for orthopedic applications. *Bioact Mater* 2018; 3: 1–18. DOI: [10.1016/j.bioactmat.2018.01.001](https://doi.org/10.1016/j.bioactmat.2018.01.001).